Evolution of the turbulent energy spectrum and length scale in Kolmogorov flow from direct numerical simulations

Kinga Andrea Kovács* and Gergely Kristóf*
Corresponding author: kingaandrea.kovacs@edu.bme.hu
*Department of Fluid Mechanics, Faculty of Mechanical Engineering, Budapest University of Technology and Economics, Műegyetem rkp. 3., H-1111 Budapest, Hungary

Abstract: Most standard engineering turbulence models rely on equilibrium assumptions, utilizing turbulent kinetic energy and its dissipation rate to characterize complex flows. However, the applicability of these two-parameter models to non-stationary, externally forced turbulence remains an open question. This study investigates the non-equilibrium dynamics of pulsating Kolmogorov flow using direct numerical simulation (DNS) to assess how accurately instantaneous turbulent states can be modeled under time-dependent forcing. Phase-averaged turbulent energy spectra are extracted and compared against Pope's model spectrum throughout the excitation cycle. Results indicate that at a non-dimensional forcing frequency of 0.79, the DNS spectrum aligns well with Pope's model spectrum. Furthermore, the integral length scale exhibits a strong periodic dependence with a distinct phase lag during its decay, while oscillating around a mean value dictated by the geometric constraints of the domain. Finally, an optimized geometric scaling approximation used to reconstruct the three-dimensional radial spectrum from one-dimensional spanwise data is evaluated. While the approximate spectrum slightly differs from the exact radial spectrum at high wavenumbers, it still successfully captures the overall energy distribution and conserves kinetic energy.

Keywords: direct numerical simulation, Kolmogorov flow, turbulence modeling, turbulent energy spectrum, turbulent length scale.

1. Introduction

Most fluid flows encountered in engineering and nature are turbulent. The aerodynamic flow past cars and aircraft, the hydrodynamics of ships, and even the mixing of sugar in a cup of coffee are all governed by turbulence. Despite its ubiquity, the fluid mechanics community still lacks a complete and universally accepted definition of turbulence. Instead, turbulent flows are commonly described through a set of characteristic features [1]:

- time-dependence,
- enhanced diffusivity,
- continuum phenomenon,
- three-dimensionality,
- dissipation,
- irregularity,
- large Reynolds numbers.

A central statistical quantity of turbulence is the distribution of kinetic energy across scales, represented by the turbulent energy spectrum. According to the classical Richardson cascade [2], kinetic energy is

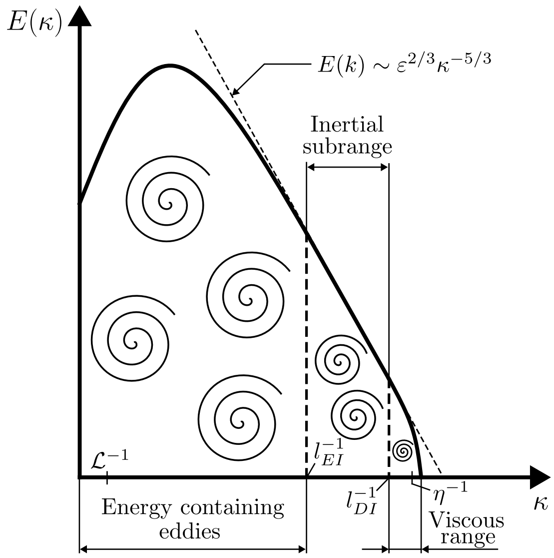

Figure 1: Schematic representation of the turbulent energy spectrum.

injected at large scales, where the flow contains the most energetic eddies. These eddies are unstable and successively break down into smaller structures, transferring energy toward increasingly small scales until it is eventually dissipated by viscosity.

Following [1] and [3], the energy spectrum can be divided into three distinct ranges (Fig. 1):

1. *Energy containing eddies:* the largest eddies, characterized by an integral length scale $\mathcal{L}$, where energy is introduced into the flow.
2. *Inertial subrange:* the intermediate scales, where energy transfer occurs with negligible viscous effects. In this region, the spectrum follows Kolmogorov's well-known $-5/3$ law [4].
3. *Viscous range:* the smallest scales ($l < l_{\mathrm{DI}}$), where viscosity removes kinetic energy. The smallest dynamically relevant length scale is the Kolmogorov scale η.

The spectrum spans scales from $\mathcal{L}$ at the low-wavenumber end to η at the high-wavenumber end. Their ratio ($\mathcal{L}/\eta$) grows with the Reynolds number as $\mathcal{L}/\eta \sim \mathrm{Re}^{3/4}$. Thus, at high Reynolds numbers, turbulence exhibits an exceptionally broad range of dynamically active scales, making the energy spectrum a key diagnostic in both theoretical and computational studies of turbulent flows.

To investigate these dynamics, we employ direct numerical simulation (DNS) of Kolmogorov flow. This idealized setup, introduced in the late 1950s, has become a widely used model for studying fundamental aspects of hydrodynamic stability, transition, and turbulence [5], with its steady, three-dimensional turbulent regime extensively characterized in classic studies [6]. While most previous studies employ a steady, spatially periodic forcing, we consider a time-dependent forcing term $f(y,t)$. We evaluate the resulting energy spectra, compare them with Pope's model spectrum [3], and analyze the evolution of the integral length scale.

Most engineering turbulence models, including standard two-equation closures, rely exclusively on two scalar quantities, for instance: the turbulent kinetic energy k and its dissipation rate ε. Pope's analytical model spectrum is built precisely on these two parameters, assuming that the entire spectral distribution can be reconstructed from k and ε together with universal correction functions. However, this assumption is fundamentally rooted in equilibrium turbulence theory and its applicability to non-stationary, externally forced flows remains an open question.

The primary objective of the present study is therefore to assess how accurately Pope's two-parameter model spectrum reproduces the temporally evolving energy spectrum obtained from DNS of pulsating

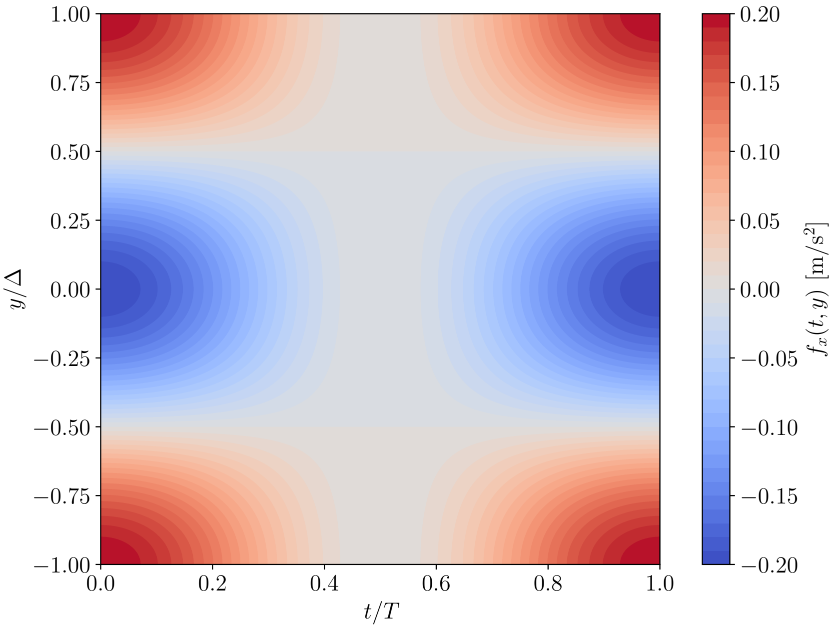

Figure 2: The applied body force.

Kolmogorov flow. We directly evaluate whether the instantaneous turbulence state – as represented by the DNS spectrum – can indeed be described solely by k and ε under time-dependent forcing.

Furthermore, because obtaining the full three-dimensional radial spectrum is often unfeasible in many practical and experimental scenarios [7], we evaluate a geometric mapping designed to reconstruct the three-dimensional spectrum from one-dimensional spanwise data. While Batchelor's well-known formula [8] provides a formal route for reconstructing the radial spectrum, it requires numerical differentiation, which can amplify noise and reduce the robustness of the reconstruction. The current mapping, on the other hand, utilizes a linear geometric scaling with an optimized constant of $\alpha = 1.6309$, while conserving the turbulent kinetic energy. By plotting this reconstructed spectrum alongside the true three-dimensional DNS spectrum and Pope's analytical model, we perform a time-resolved evaluation of both approaches. The outcome provides vital insight into the validity range of equilibrium-based turbulence models in non-stationary flows, while simultaneously establishing the physical limits of one-dimensional-to-three-dimensional spectral reconstruction techniques under time-dependent forcing.

2. Direct numerical simulation

The DNS was carried out using the open-source spectral element solver NEK5000 [9]. In the spectral element method, the solution is represented within each element by high-order tensor-product polynomials with Gauss-Lobatto-Legendre (GLL) nodes. The computational domain was a cube of side length $2\Delta = 0.05$ m with periodic boundary conditions in all directions. Each coordinate was discretized using 8 spectral elements, each containing 16 GLL points for the velocity field, resulting in a resolution of 128 points per direction. The simulation was initialized with a randomly perturbed velocity field. The time step was chosen adaptively to maintain a maximum Courant number of 0.5 and the simulation was run for 119.15 s. The fluid density was set to $\rho = 1000\,\mathrm{kg/m^3}$, and the dynamic viscosity to $\mu = 0.001\,\mathrm{kg/(m \cdot s)}$.

The x-direction body force was implemented using a local acceleration subroutine (`userf`). The time-dependent forcing (which is shown in Fig. 2) took the form:

$$f_x(t, y) = -\hat{f}\cos(\kappa_1 y)\left(\cos\left(\omega_e t\right) + 1\right) = -0.1\cos\left(\frac{\pi}{\Delta}y\right)\left(\cos\left(\frac{2\pi}{T}t\right) + 1\right), \tag{1}$$

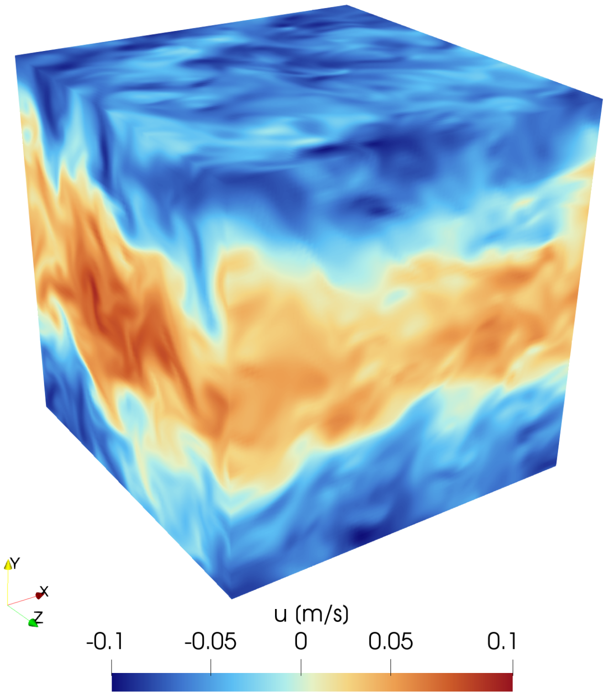

Figure 3: Instantaneous streamwise velocity field at $t = 119.15$ s.

where $\hat{f}$ [m/s^2] is the forcing amplitude, κ_1 [1/m] is the excitation wavenumber (the flow was excited in the first mode), ω_e [1/s] is the excitation frequency, and $T = 4$ s is the time period. For post-processing, the velocity field was interpolated from the original grid onto a uniform mesh with 256^3 nodes using 15$^{\text{th}}$-degree Lagrange polynomials. During post-processing horizontal averages were taken over x-z planes. The instantaneous streamwise velocity field at $t = 119.15$ s is shown in Fig. 3.

3. Turbulent energy spectrum

3.1 Spectral analysis

The radial turbulent energy spectrum $E(\kappa)$ was obtained from the instantaneous velocity fields using a three-dimensional discrete Fourier transform, followed by integration of the spectral energy over spherical shells of radius $\kappa = |\boldsymbol{\kappa}|$. This representation compactly describes the distribution of kinetic energy across spatial scales. The evolution of the turbulent energy spectrum – displaying three representative cycles – is shown in Fig. 4.

To enhance statistical convergence, phase-averaging was performed over the total number of excitation periods, yielding a single representative cycle. The evolution of the phase-averaged turbulent energy spectrum is shown in Fig. 5. Based on Fig. 5 it can be seen that the flow exhibits maximum energy in the early phase of the cycle, followed by a global decay across all scales as the phase angle increases. A wave-like propagation of energy is observed in the spectrum, with the maxima and minima appearing at high wavenumbers after a distinct time delay.

3.2 Pope's model equation

To evaluate the non-equilibrium effects of the time-varying excitation, the DNS results were compared against the analytical model proposed by Pope [3]:

$$E(\kappa) = C\,\varepsilon^{2/3}\kappa^{-5/3}\,f_L(\kappa L)\,f_\eta(\kappa\eta), \tag{2}$$

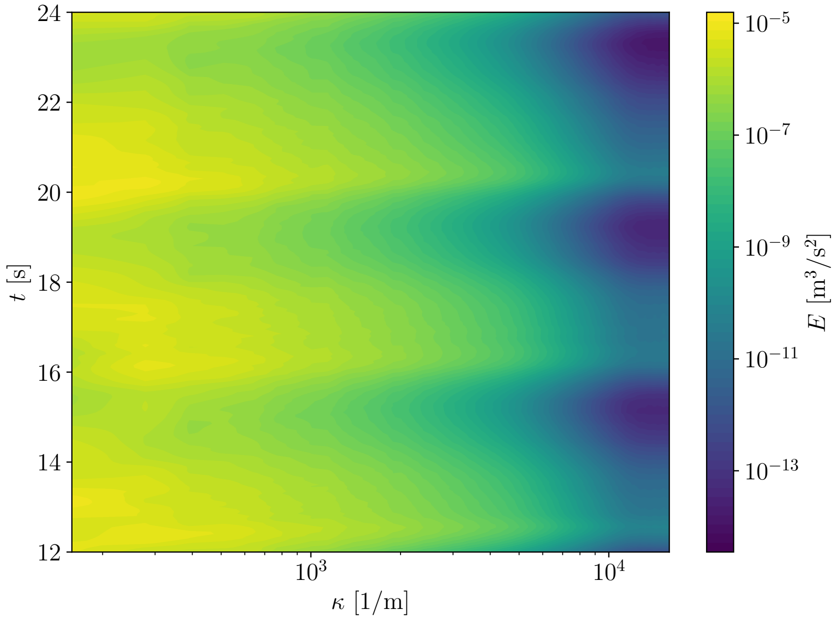

Figure 4: Evolution of the turbulent energy spectrum.

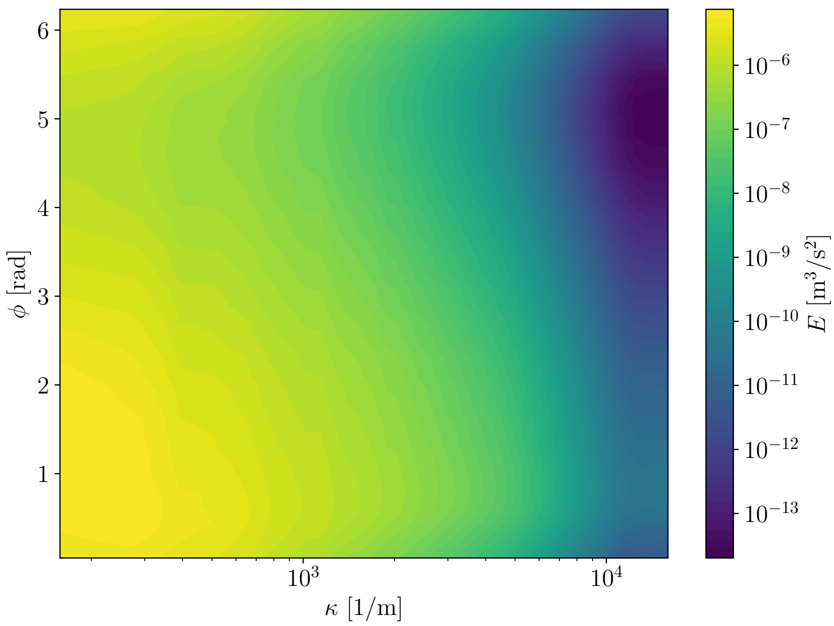

Figure 5: Evolution of the turbulent energy spectrum in phase-averaged representation.

where the large-scale correction function:

$$f_L(\kappa L) = \left(\frac{\kappa L}{\left[(\kappa L)^2 + c_L\right]^{1/2}} \right)^{5/3+p_0}, \tag{3}$$

controls the shape of the energy-containing range and satisfies $f_L \to 1$ for $\kappa L \gg 1$. The small-scale correction:

$$f_\eta(\kappa\eta) = \exp\left[-\beta \left(\left[(\kappa\eta)^4 + c_\eta^4\right]^{1/4} - c_\eta \right)\right], \tag{4}$$

determines the form of the dissipation range and approaches unity for $\kappa\eta \ll 1$. The model constants used

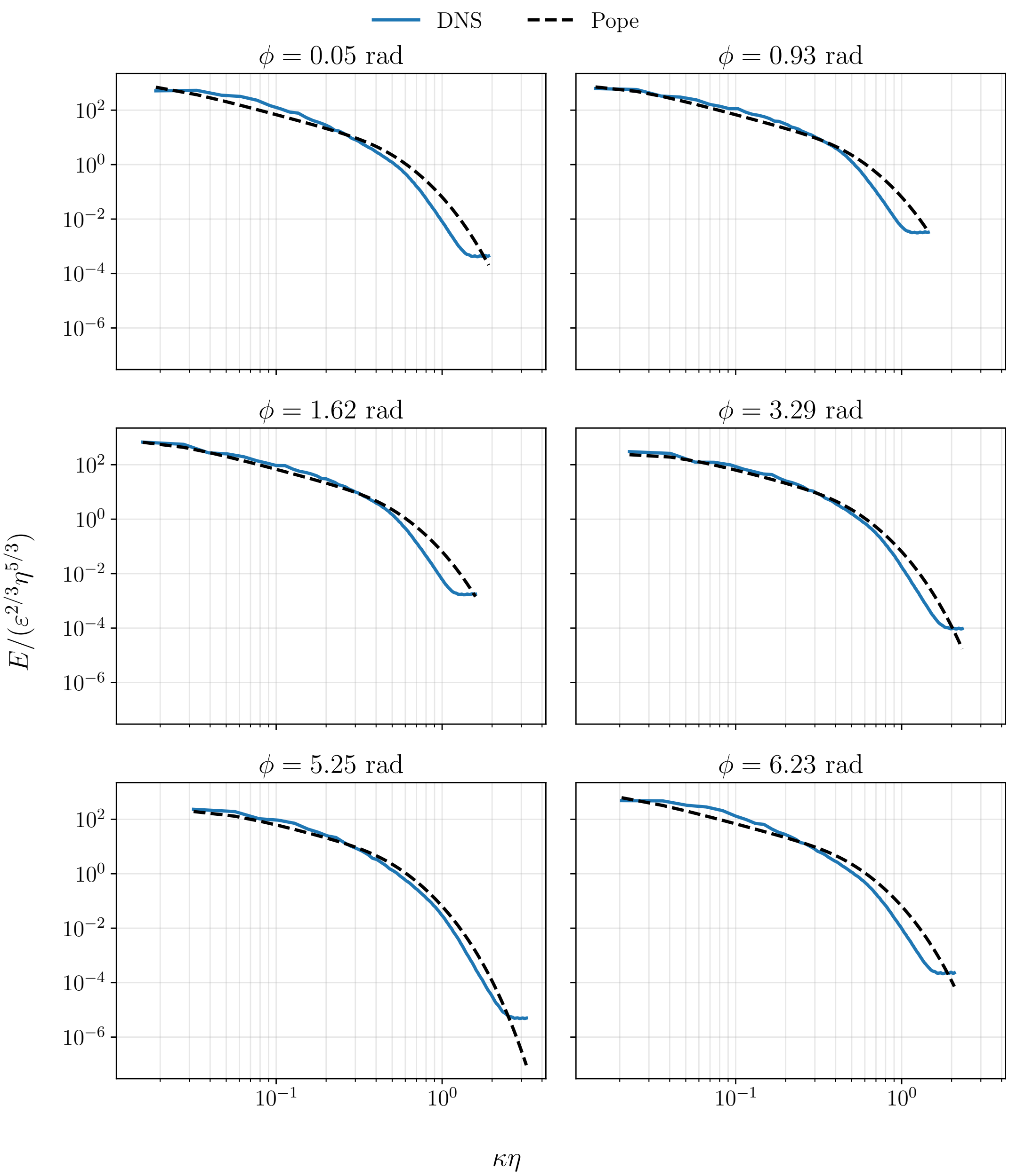

Figure 6: Comparison of the radial energy spectrum with Pope's model spectrum at different phase angles.

in this study are [3]:

$$C = 1.5, \quad p_0 = 2, \quad \beta = 5.2, \quad c_L = 6.78, \quad c_\eta = 0.4. \tag{5}$$

To evaluate Pope's analytical spectrum, the required length scales were computed directly from the turbulent kinetic energy and the dissipation rate obtained from the DNS. The integral length scale was computed as:

$$L = \frac{k^{3/2}}{\varepsilon}. \tag{6}$$

This length scale characterizes the size of the energy-containing eddies. The small-scale (dissipative)

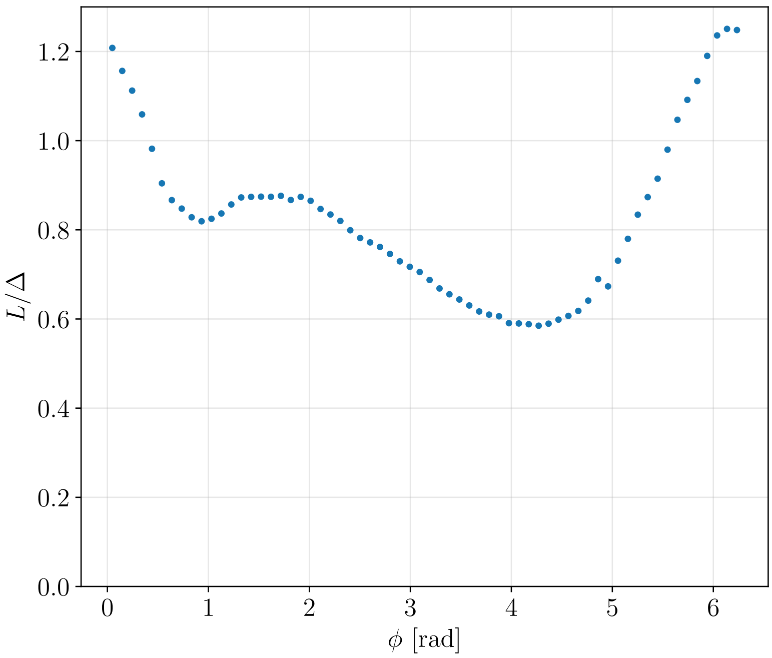

Figure 7: Length scale evolution in pulsating Kolmogorov flow.

length scale was computed from:

$$\eta = \left(\frac{\nu^3}{\varepsilon}\right)^{1/4}, \tag{7}$$

consistent with Kolmogorov theory. With L and η determined, Pope's model spectrum was evaluated on the same wavenumber grid as the DNS spectrum for direct comparison. The comparison of the spectrum with Pope's model spectrum at different phase angles is shown in Fig. 6.

Based on Fig. 6, the spectrum calculated from the DNS data shows good agreement with the model spectrum of Pope. The degree of agreement may be influenced by the non-dimensional forcing frequency $\varOmega$, which characterizes the excitation frequency relative to a forcing-based inertial frequency. The latter is defined a priori as:

$$\omega_t = \sqrt{\frac{\hat{f}}{\Delta}}, \tag{8}$$

corresponding to the reciprocal of the inertial time scale:

$$\tau_t = \omega_t^{-1} = \sqrt{\frac{\Delta}{\hat{f}}}. \tag{9}$$

This time scale may be interpreted as the characteristic time over which the forcing acceleration $\hat{f}$ induces motion over the length scale Δ. In the present case, the non-dimensional forcing frequency is:

$$\varOmega = \frac{\omega_e}{\omega_t} = \frac{\frac{2\pi}{T}}{\sqrt{\frac{\hat{f}}{\Delta}}} = 0.79. \tag{10}$$

3.3 Length scale evolution

The evolution of the integral length scale can be seen in Fig. 7, where Δ (half side length of the computational domain) acts as a geometric filter size. The authors already utilized this geometric filter size in developing a modified geometry-informed eddy viscosity formulation for the standard k-ε model [10]. Based on Fig. 7, it can be seen that the normalized integral length scale L/Δ exhibits a strong periodic dependency, oscillating between approximately 0.6 and 1.3.

A positive correlation can be observed between the driving force and the turbulent length scale. The maximum value of L is around $\phi = 0$ rad, where the sinusoidal excitation actually reaches its maximum. On the other hand, the sinusoidal excitation reaches its minimum at $\phi = \pi$ rad, however, the length scale continues to decay, reaching its global minimum at approximately $\phi \approx 4.27$ rad. This delay between the macroscopic forcing and the turbulence statistics is consistent with phenomena observed in other unsteady turbulent flows [11]. Furthermore, the fact that L/Δ oscillates mostly around unity – $(L/\Delta)_{\text{mean}} = 0.83$ – means that the energy-containing structures are physically constrained by the domain itself.

3.4 Evaluating a geometric scaling approximation

In many practical and experimental scenarios, obtaining the full three-dimensional radial spectrum is unfeasible. Instead, one-dimensional spectra are often measured along specific directions. To reconstruct the three-dimensional spectrum from one-dimensional data, a geometric mapping can be employed. We seek a differentiable, monotone transformation $\kappa_r = f(\kappa_z)$ such that the energy contained in corresponding infinitesimal intervals is conserved $(E_r(\kappa_r)\,\mathrm{d}\kappa_r = E_z(\kappa_z)\,\mathrm{d}\kappa_z)$. This implies that:

$$E_r(\kappa_r) = \frac{E_z(\kappa_z)}{f'(\kappa_z)}. \tag{11}$$

The simplest transformation (which is part of an ongoing research) assumes a linear geometric scaling, $f(\kappa_z) = \alpha\kappa_z$, with an optimized constant $\alpha = 1.6309$, while conserving the turbulent kinetic energy. The approximate radial spectrum preserved the turbulent kinetic energy within less than 1%, and the reconstructed dissipation values demonstrated excellent agreement with the true DNS field, yielding a mean-squared logarithmic error of just 8.9%. The approximate radial spectrum is calculated as:

$$E_{r,\text{approx}} = \frac{E_z}{\alpha}, \tag{12}$$

where E_z is the one-dimensional spanwise spectrum obtained from the DNS. The directional wavenumber is scaled as:

$$\kappa_{r,\text{approx}} = \alpha\kappa_z. \tag{13}$$

The comparison of the reconstructed spectrum with the true three-dimensional DNS spectrum and Pope's model spectrum is shown in Fig. 8. As illustrated, the reconstructed mapping captures the general shape of the energy distribution well. Although it exhibits slight deviations from the true three-dimensional spectrum – particularly at high wavenumbers – the approximation overall provides a highly practical, noise-free reconstruction of the radial spectrum. Nonetheless, it should be tested in more anisotropic flows to fully evaluate its general applicability.

4. Conclusion

In this study, we investigated the dynamics of pulsating Kolmogorov flow using DNS data. Our results showed that the turbulent response does not adjust instantaneously to the excitation cycle. Instead, the integral length scale reaches its minimum only after the forcing has passed its minimum, indicating a finite response time associated with the inertia of the bulk flow. Consistent with this behavior, a positive correlation was observed between the driving force and the turbulent length scale.

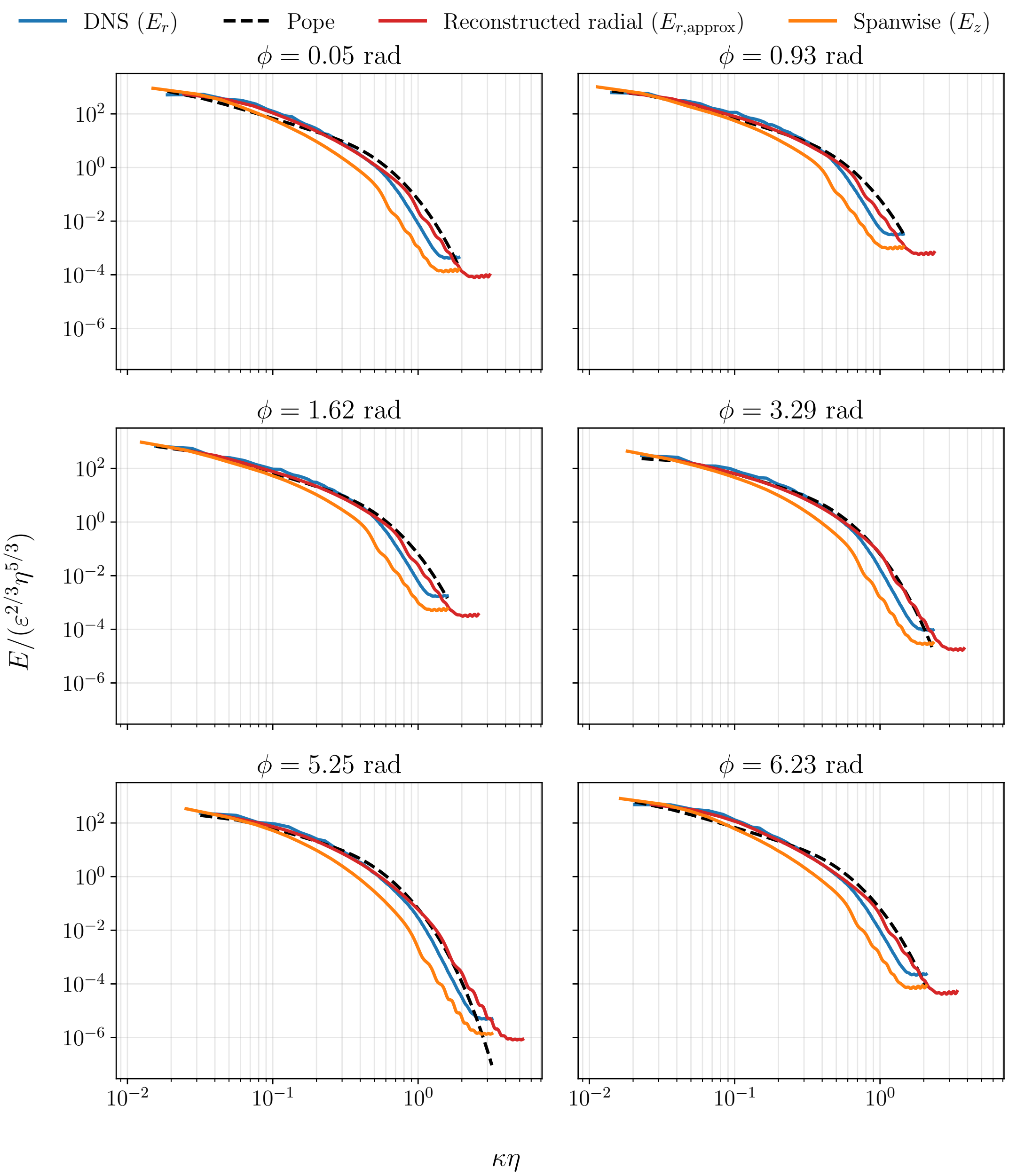

Figure 8: Comparison of the approximate radial spectrum with the true radial spectrum and Pope's model spectrum at different phase angles (the original spanwise spectrum is also shown).

Spectral analysis revealed that the energy distribution aligns remarkably well with Pope's model spectrum. At a dimensionless excitation frequency of $\Omega = 0.79$, a two-parameter spectrum based on k and ε satisfactorily described the observed temporal evolution of the turbulent kinetic energy. From an engineering perspective, this robustness is highly encouraging, as it suggests that standard two-equation closures may remain valid for mildly non-stationary flows where the turbulence cascade adjusts sufficiently fast to the macroscopic forcing. Furthermore, a wave-like propagation of energy was evident, with spectral maxima and minima appearing at high wavenumbers after a distinct time delay.

Our evaluation of a geometric scaling approximation ($\alpha = 1.6309$) demonstrated that a one-dimensional spanwise spectrum can be effectively mapped to reconstruct the three-dimensional radial spectrum. While there were some deviations at high wavenumbers, it still successfully captured the kinetic energy and dissipation variations. This finding is particularly relevant for experimental studies where only one-dimensional spectral data may be available, providing a practical method for estimating the full three-dimensional energy distribution. The approximation's performance in more anisotropic flows should be investigated in future studies to assess its general applicability.

The observation that L/Δ oscillated primarily around unity confirmed that the energy-containing eddies are physically constrained by the computational domain. These findings highlight the need for geometry-aware turbulence models, which serves as the main objective for our current research.

Acknowledgements

The research reported in this paper is part of project no. **K146158**, implemented with the support provided by the Ministry of Culture and Innovation of Hungary from the National Research, Development and Innovation Fund, financed under the **OTKA K 23** funding scheme. Supported by the **EKÖP-25-3-BME-54** University Research Scholarship Program of the Ministry for Culture and Innovation from the source of the National Research, Development, and Innovation Fund. We acknowledge the Digital Government Development and Project Management Ltd. for awarding us access to the **Komondor HPC facility** based in Hungary.

References

[1] D. C. Wilcox. *Turbulence modeling for CFD*. DCW Industries, 1993.

[2] L. F. Richardson. *Weather prediction by numerical process*. Cambridge University Press, 1922.

[3] S. B. Pope. *Turbulent flows*. Cambridge University Press, 2000.

[4] A. N. Kolmogorov. The local structure of turbulence in incompressible viscous fluid for very large Reynolds numbers. *Proceedings of the Royal Society of London. Series A: Mathematical and Physical Sciences*, 434(1890):9–13, 1991.

[5] E. D. Fylladitakis. Kolmogorov flow: Seven decades of history. *Journal of Applied Mathematics and Physics*, 6(11):2227–2263, 2018.

[6] V. Borue and S. A. Orszag. Numerical study of three-dimensional Kolmogorov flow at high Reynolds numbers. *Journal of Fluid Mechanics*, 306:293–323, 1996.

[7] G. Comte-Bellot and S. Corrsin. Simple Eulerian time correlation of full-and narrow-band velocity signals in grid-generated, 'isotropic' turbulence. *Journal of Fluid Mechanics*, 48(2):273–337, 1971.

[8] G. K. Batchelor. *The theory of homogeneous turbulence*. Cambridge University Press, 1953.

[9] P. Fischer, J. Lottes, and H. Tufo. Nek5000. *Tech. Rep*, Argonne National Laboratory (ANL), Argonne, IL (United States), 2007. Available: https://nek5000.mcs.anl.gov.

[10] G. Kristóf, K. A. Kovács, T. Kalmár-Nagy, and M. Balogh. A geometry-informed eddy viscosity formula with sublinear geometric scale dependence. *Physics of Fluids*, 37(12), 2025.

[11] A. Scotti and U. Piomelli. Numerical simulation of pulsating turbulent channel flow. *Physics of Fluids*, 13(5):1367–1384, 2001.